

Supplementary Material for

“Twist-stacked 2D bilayer Fe_3GeTe_2 with tunable magnetism”

Dong Chen ^a, Wei Sun ^b, Wenxuan Wang ^b, Xiaoning Li ^c, Hang Li ^{b,*}, Zhenxiang Cheng ^{c,*}

^a College of Physics and Electronic Engineering, Xinyang Normal University, Xinyang, 464000, P. R. China

^b School of Physics and Electronics, Henan University, Kaifeng, 475004, P. R. China. E-mail: hang.li@vip.henu.edu.cn (H. Li)

^c Institute for Superconducting and Electronic Materials, Australian Institute of Innovative Materials, University of Wollongong, Wollongong, NSW 2500, Australia. E-mail: cheng@uow.edu.au (Z. X. Cheng)

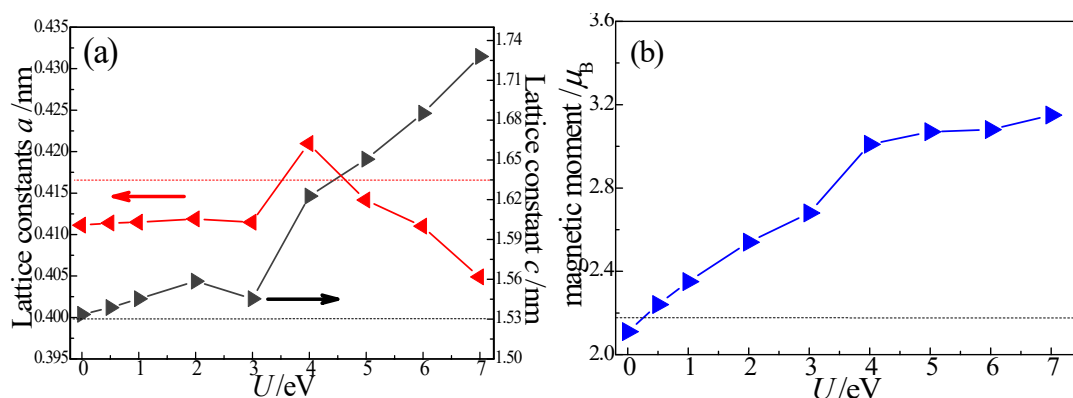


Fig. S1 Ground-state lattice parameters a (red-line) and c (black-line) (a) and the average magnetic moment m (blue line) of Fe ions in the bulk Fe_3GeTe_2 (FGT) as a function of U (b). Dashed lines indicate the experimental data.

The relationship between the Hubbard U and the structural properties of bulk Fe_3GeTe_2 (FGT) is presented in Fig. S1. The lattice constant a and magnetic moment m agree well with the experimental data when $U = 0.5$ ^[1]. The calculated lattice constant c is also consistent with the experimental data. The relative error is lower than 1.9% when $U = 0.5$, which is within the general accuracy of the GGA + PBE + U scheme (usually less than 3%). On the one hand, the agreement between our results and the experimental data supports the reliability of our calculation. On the other hand, the effective U of Fe-3d orbital for the FGT material should not be too large ^[2, 3]. $U = 2.0$ or 6.0 lead to an overestimation of the magnetic moments for FGT monolayer ^[3].

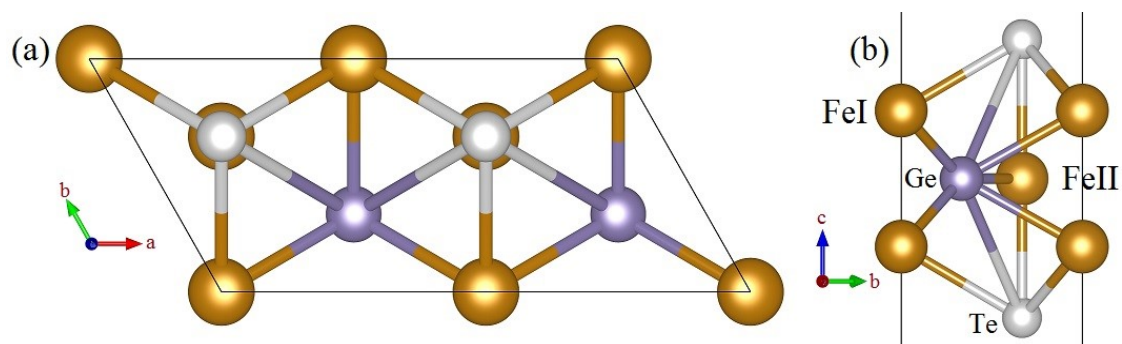


Fig. S2 Top view (a) and side view (b) of the 2D structures of the monolayer FGT.

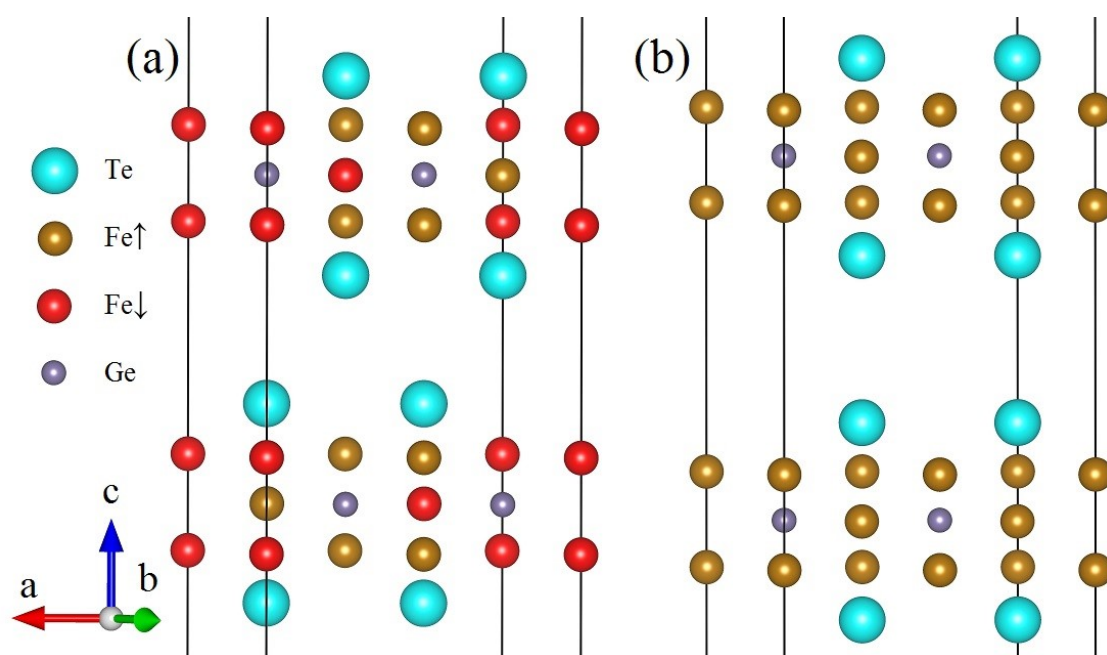


Fig. S3 Side views of (a) the 0° and (b) the 180° twist-stacked Fe_3GeTe_2 bilayers. [the yellow and red balls represent the Fe (spin-up) and Fe (spin-down) ions, respectively].

Table S1 Zero-temperature Gibbs free energy (enthalpy) differences ΔG per Fe atom among the FM, AFM, and FiM configurations for the FGT monolayer and bilayers

Magnetic orders of monolayer	Spin states	$\Delta G /$ meV	Magnetic orders of bilayers	Spin states	$\Delta G /$ meV	
					0° bilayer	180° bilayer
1-FM	↑↑↑↑↑↑	0	1- FM	↑↑↑↑↑↑↑↑↑↑	14.33	0.00
2-AFM	↓↓↓↑↑↑	72.47	2-AFM	↑↑↓↓↑↓↑↓↑↓↓↑	123.69	71.74
3-AFM	↓↓↑↑↑↓	104.89	3-AFM	↑↓↑↓↑↑↓↓↑↓↓↑	113.17	70.95
4-AFM	↑↓↑↑↓↓	160.18	4-AFM	↑↓↓↑↑↓↑↓↑↑↓↓	5.24	115.75
5-AFM	↑↓↓↑↓↑	160.18	5-AFM	↑↑↓↓↑↓↓↑↑↓↑↓	74.83	109.41
6-FiM	↓↑↑↑↑↑	74.00	6-AFM	↑↓↑↓↑↓↓↑↑↑↓↓	81.16	83.57
7-FiM	↑↓↑↑↑↑	73.99	7-AFM	↑↓↑↓↑↓↓↑↑↓↑↓	122.18	71.74
8-FiM	↑↑↓↑↑↑	12.69	8-AFM	↓↓↓↓↑↑↑↑↑↑↓	0.00	77.08
9-FiM	↑↑↑↓↑↑	74.01	9-AFM	↑↑↑↑↓↓↑↓↑↓↓↓	77.81	73.51
10-FiM	↑↑↑↑↓↑	73.99	10-AFM	↑↓↑↓↑↑↓↓↓↓↑↑	39.52	35.23
11-FiM	↑↑↑↑↑↓	12.70	11-AFM	↓↓↓↑↑↑↓↑↓↑↑↑	38.84	36.87
12-FiM	↓↓↑↑↑↑	72.47	12-AFM	↑↑↓↓↑↑↑↑↓↑↓↑	14.37	72.44
13-FiM	↓↑↓↑↑↑	74.00	13-AFM	↑↑↓↓↓↑↑↑↓↑↑↑	39.55	42.13
14-FiM	↓↑↑↑↓↑	94.76	14-FiM	↓↓↑↑↑↑↓↓↓↑↑↑	40.91	36.39
15-FiM	↓↑↑↑↑↓	74.01	15-FiM	↑↑↑↑↓↑↑↑↓↓↓↓	89.90	42.12
16-FiM	↑↓↓↑↑↑	73.99	16-FiM	↑↓↑↓↓↑↓↑↓↑↑↓	14.39	10.93
17-FiM	↑↑↓↓↑↑	74.01	17-FiM	↑↑↓↑↑↓↑↑↑↑↑↓	38.84	35.23
18-FiM	↑↑↓↑↑↓	12.69	18-FiM	↑↑↓↓↑↓↑↑↑↑↑↓	74.52	36.39
19-FiM	↑↓↑↑↓↑	148.51	19-FiM	↑↓↑↓↑↓↑↑↑↑↑↓	39.52	36.39
20-FiM	↑↑↑↑↓↓	73.99	20-FiM	↑↓↑↑↑↓↑↑↑↑↑↓	40.23	36.39
			21-FiM	↑↑↓↓↑↑↑↑↑↑↓	82.61	35.49
			22-FiM	↑↓↑↓↑↑↑↑↑↑↓	38.82	36.86
			23-FiM	↑↓↑↓↑↑↑↑↑↑↓	14.32	108.98
			24-FiM	↑↓↑↓↑↓↑↓↑↑↑↑	85.39	78.06
			25-FiM	↑↑↓↓↑↓↑↓↑↑↑↓	80.70	77.78
			26-FiM	↑↑↓↓↑↓↑↓↑↑↑↑	75.48	115.75
			27-FiM	↑↑↓↓↑↓↑↓↑↑↑↑	179.08	71.86
			28-FiM	↑↑↓↓↑↓↑↑↑↑↑↑	82.61	36.39
			29-FiM	↑↑↓↓↑↑↑↑↑↑↓	74.54	36.86
			30-FiM	↑↓↑↑↑↑↓↑↑↑↓	40.01	74.25

The Gibbs energy difference $\Delta G = G_I - G_L$ of the FGT monolayer is calculated and listed in Table S1. The subscripts I and L indicate a given magnetic order (ferromagnetic FM, antiferromagnetic AFM, ferrimagnetic FiM) and the magnetic order with the lowest energy, respectively. The results show that the FGT monolayer has FM order, which are in agreement with the previous results [4-6]. The calculated magnetic moments are $2.51 \mu_B/\text{Fe}$ (FeI atom), $1.66 \mu_B/\text{Fe}$ (FeII atom), and $2.22 \mu_B/\text{Fe}$ (average value). These results are in good agreement with the experimental data ($1.625 \mu_B/\text{Fe}$ [4]), the theoretical results ($2.5 \mu_B/\text{Fe}$ for the FeI atoms [5], $1.5 \mu_B/\text{Fe}$ for the FeII atom [5]), and the average magnetic moment ($1.53 \mu_B/\text{Fe}$ [6], $1.58 \mu_B/\text{Fe}$ [7]). Our results of the magnetic moments for the FGT monolayer are larger than the experimental data [4, 8]. Local density approximation (LDA)+ U , GGA, and GGA+ U functionals often yield average magnetic moments of Fe greater than $2 \mu_B/\text{Fe}$ [2, 9, 10]. Therefore, the calculated results do not affect our qualitative analysis of magnetism in the 2D FGT systems. As shown in Fig. S2, the detailed fractional coordinates of the Fe atoms of the monolayer FGT are Fe1 (0, 0, 0.6606), Fe2 (0, 0, 0.5841), Fe3 (0.1667, 0.6667, 0.6223), Fe4 (0.5, 0, 0.6606), Fe5 (0.5, 0, 0.5841), and Fe6 (0.6667, 0.6667, 0.6223).

Table S1 also shows the Gibbs free energy difference ΔG of the twist-stacked FGT bilayers. Each magnetic bilayer includes one FM, twelve AFM, and seventeen FiM magnetic orders. The calculated results indicate that the most stable structures of the 0° and 180° bilayers are the 8-AFM and FM phases, respectively. The fractional coordinates of different Fe atoms of the 0° bilayer are Fe1 (0, 0, 0.3394), Fe2 (0, 0, 0.6606), Fe3 (0, 0, 0.5841), Fe4 (0, 0, 0.4159), Fe5 (0.3333, 0.3333, 0.3777), Fe6 (0.1667, 0.6667, 0.6223), Fe7 (0.5, 0, 0.3394), Fe8 (0.5, 0, 0.6605), Fe9 (0.5, 0, 0.5841), Fe10 (0.5, 0, 0.4159), Fe11 (0.8333, 0.3333, 0.3776), and Fe12 (0.6667, 0.6667, 0.6223). For the 180° bilayer, the coordinates of Fe are Fe1 (0, 0, 0.4018), Fe2 (0, 0, 0.3279), Fe3 (0.1667, 0.6667, 0.3649), Fe4 (0, 0, 0.6721), Fe5 (0, 0, 0.5981), Fe6 (0.1667, 0.6667, 0.6351), Fe7 (0.5, 0, 0.4018), Fe8 (0.5, 0, 0.3279), Fe9 (0.6667, 0.6667, 0.3649), Fe10 (0.5, 0, 0.6721), Fe11 (0.5, 0, 0.5982), and Fe12 (0.6667, 0.6667, 0.6351).

Table S2 the average bond length BL (Å) of the freestanding FGT bilayer

Bonds	0° FGT bilayer		180° FGT bilayer	
	Upper layer	Lower layer	Upper layer	Lower layer
FeI--FeII	2.6528 (Å)	2.6175 (Å)	2.6184 (Å)	2.6187 (Å)
FeI--Te	2.6764 (Å)	2.6865 (Å)	2.6829 (Å)	2.6828 (Å)
FeI--Ge	2.6504 (Å)	2.6185 (Å)	2.6181 (Å)	2.6179 (Å)
FeII--Te	2.6481 (Å)	2.6243 (Å)	2.6178 (Å)	2.6177 (Å)
FeII--Ge	2.3114 (Å)	2.3044 (Å)	2.3042 (Å)	2.3041 (Å)

The average bond lengths (BLs) among the FeI, FeII, Ge, and Te ions are listed in Table S2, where the upper and lower layers are illustrated in Fig. 1 of the main text. For the 0° case, the average BLs of the upper layer are slightly longer than those of the lower layer. When the rotation angle changes to 180°, the symmetry of our FGT bilayer is changed, and the BLs of the lower and upper layers tend to be the same. Variation of bond length significantly changes the electronic environment and charge transfer around the FeI and FeII atoms, thus changing the electronic structure and magnetism of the 2D bilayer. These results reflect that the “twist-stacking” scheme is a practical way to manipulate the magnetic and electronic properties of 2D FGT bilayers.

References

- [1] J. Y. Yi, H. L. Zhuang, Q. Zou, Z. M. Wu, G. X. Cao, S. W. Tang, S. A. Calder, P. R. C. Kent, D. Mandrus and Z. Gai, Competing Antiferromagnetism in a Quasi-2D Itinerant Ferromagnet: Fe_3GeTe_2 , *2D Mater.*, 2017, **4**, 011005, DOI: 10.1088/2053-1583/4/1/011005.
- [2] Y. J. Deng, Y. J. Yu, Y. C. Song, J. Z. Zhang, N. Z. Wang, Z. Y. Sun, Y. F. Yi, Y. Z. Wu, S. W. Wu, J. Y. Zhu, J. Wang, X. H. Chen and Y. B. Zhang, Gate-Tunable Room-Temperature Ferromagnetism in Two-Dimensional Fe_3GeTe_2 , *Nature*, 2018, **563**, 94-99, DOI: 10.1038/s41586-018-0626-9.
- [3] H. L. Zhuang, P. R. C. Kent and R. G. Hennig, Strong Anisotropy and Magnetostriction in the Two-Dimensional Stoner Ferromagnet Fe_3GeTe_2 , *Phys. Rev. B*, 2016, **93**, 134407, DOI:

10.1103/PhysRevB.93.134407.

- [4] B. Chen, J. H. Yang, H. D. Wang, M. Imai, H. Ohta, C. Michioka, K. Yoshimura and M. H. Fang, Magnetic Properties of Layered Itinerant Electron Ferromagnet Fe_3GeTe_2 , *J. Phys. Soc. Jpn.*, 2013, **82**, 124711, DOI: 10.7566/JPSJ.82.124711.
- [5] D. Kim, S. Park, J. Lee, J. B. Yoon, S. J. Joo, T. Kim, K. J. Min, S. Y. Park, C. Kim, K. W. Moon, C. Lee, J. Hong and C. Hwang, Antiferromagnetic Coupling of van der Waals Ferromagnetic Fe_3GeTe_2 , *Nanotechnology*, 2019, **30**, 245701, DOI: 10.1088/1361-6528/ab0a37.
- [6] X. H. Hu, Y. H. Zhao, X. D. Shen, A. V. Krasheninnikov, Z. F. Chen and L. T. Sun, Enhanced Ferromagnetism and Tunable Magnetism in Fe_3GeTe_2 Monolayer by Strain Engineering, *ACS Appl. Mater. Interfaces*, 2020, **12**, 26367-26373, DOI: 10.1021/acsami.0c05530.
- [7] J. X. Zhu, M. Janoschek, D. S. Chaves, J. C. Cezer, T. Durakiewicz, F. Ronning, Y. Sassa, M. Mansson, B. L. Scott, N. Wakeham, E. D. Bauer and J. D. Thompson, Electronic Correlation and Magnetism in the Ferromagnetic Metal Fe_3GeTe_2 , *Phys. Rev. B*, 2016, **93**, 144404, DOI: 10.1103/PhysRevB.93.144404.
- [8] A. F. May, S. Calder, C. Cantoni, H. Cao and M. A. McGuire, Magnetic Structure and Phase Stability of the van der Waals Bonded Ferromagnet Fe_3GeTe_2 , *Phys. Rev. B*, 2016, **93**, 014411, DOI: 10.1103/PhysRevB.93.014411.
- [9] H. S. Wang, R. Z. Xu, C. Liu, L. Wang, Z. Zhang, H. M. Su, S. M. Wang, Y. S. Zhao, Z. J. Liu, D. P. Yu, J. W. Mei, X. L. Zou and J. F. Dai, Pressure-Dependent Intermediate Magnetic Phase in Thin Fe_3GeTe_2 Flakes, *J. Phys. Chem. Lett.*, 2020, **11**, 7313-7319, DOI: 10.1021/acs.jpcclett.0c01801.
- [10] H. J. Deiseroth, K. Aleksandrov, C. Reiner, L. Kienle and R. K. Kremer, Fe_3GeTe_2 and Ni_3GeTe_2 -Two New Layered Transition-Metal Compounds: Crystal Structures, HRTEM Investigations, and Magnetic and Electrical properties, *Eur. J. Inorg. Chem.*, 2006, **2006**, 1561-1567, DOI: 10.1002/ejic.200501020.